Non-hotspot volcano chains from small-scale sublithospheric convection (a 3D-numerical study)

Maxim D. Ballmer*[1], Jeroen van Hunen[1,2], Garrett Ito[3], Paul J. Tackley[1], Todd A. Bianco[3]

*ballmer@tomo.ig.erdw.ethz.ch; [1]Institute of Geophysics, ETH Zurich, Switzerland
[2]Dep. of Earth Sciences, University of Durham, UK; [3]SOEST, University of Hawaii, Honolulu, USA

Introduction

Fig. 1: Though aligned by plate motion, age progressions of the Pukapuka ridges (*Fig. 2*), Marshall, Cook-Austral, and Line Islands violate the predictions of the hotspot hypothesis. The radiometric ages (in Ma) collected require an alternative explanation (e. g., sublithospheric small-scale convection).

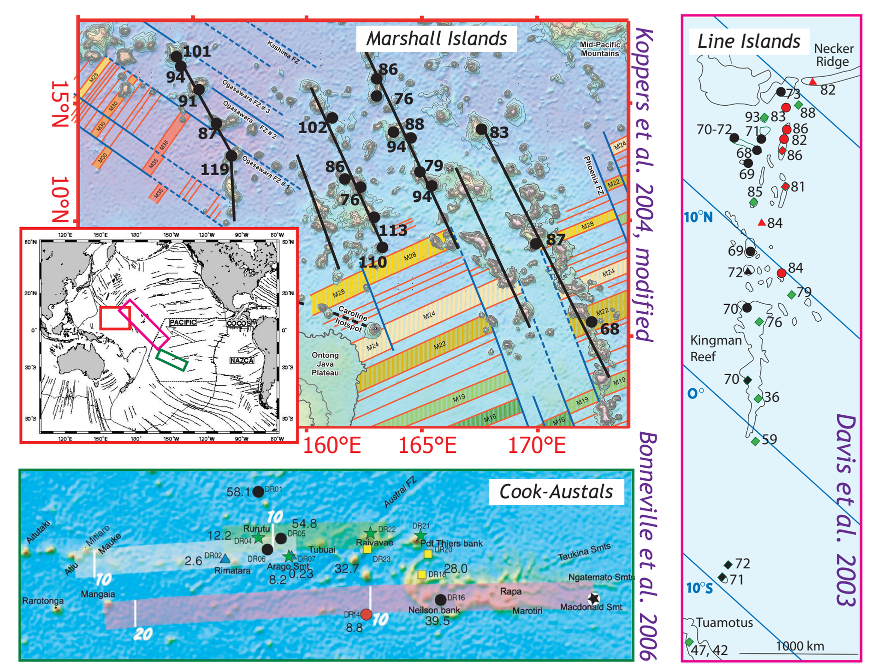

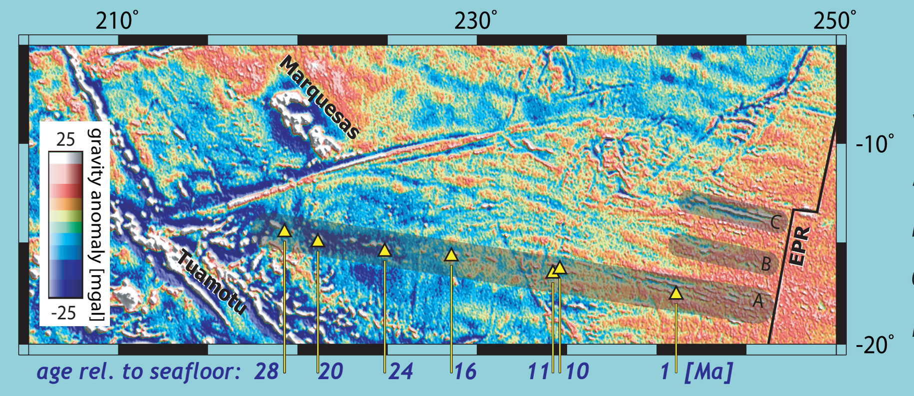

Fig. 2: Short intraplate volcanic chains in the S-Pacific aligning plate motion and gravity lineations (A: Pukapuka, B: Hotu Matua, C: Sejourn) These have been yet attributed to small-scale convection and lithospheric cracking. The first model has not been tested and validated in a 3D-numerical model yet, while the latter presumes a widely partially molten mantle.

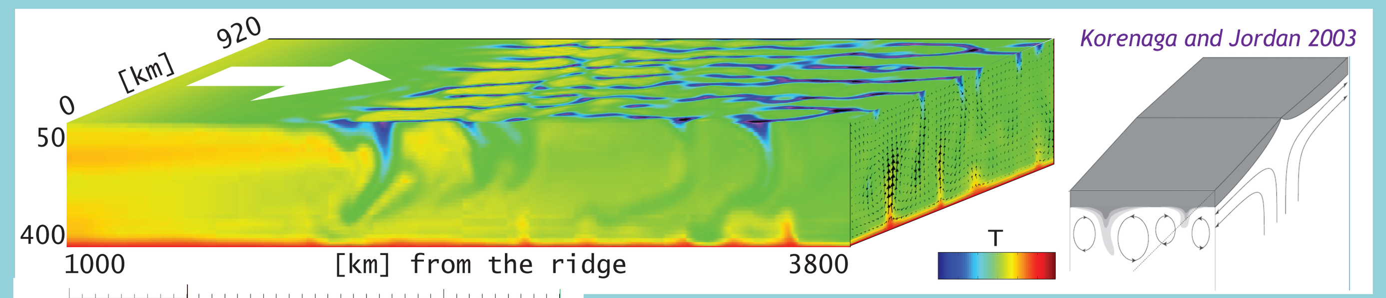

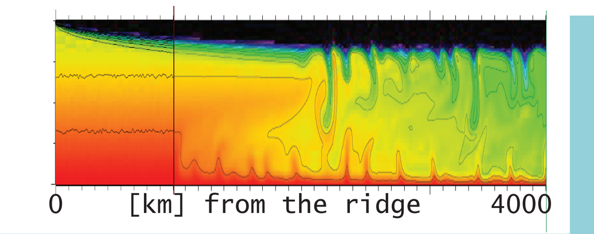

Fig. 3: Small-scale convection evolves in rolls aligning plate-motion due to instabilities of the thermal boundary layer, after growing beyond a critical thickness beneath mature seafloor.

Fig. 4: The onset of small-scale convection is usually beneath 70 Ma old oceanic lithosphere. But it is highly sensitive to mantle viscosity with an earlier onset for a weaker asthenosphere. The onset is also reduced adjacent to lateral (compositional or thermal) density heterogeneity.

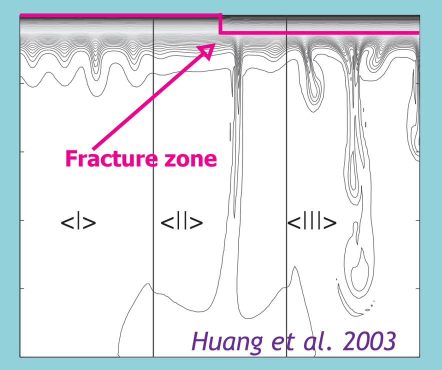

Model setup

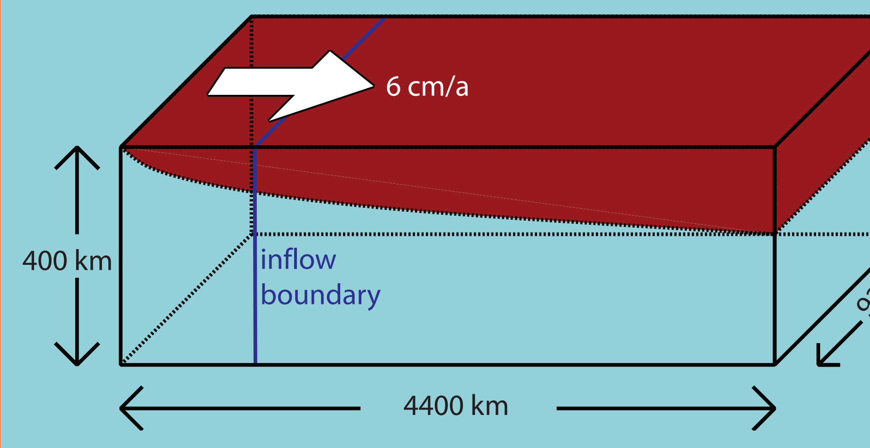

Fig. 5: Calculations are performed using the FEM-code CITCOM (Moresi and Gurnis 1996, Zhong et al. 2000) in a box of 256x48x96 elements. Thermo-chemical convection is modeled by considering Newtonian temperature- and depth-dependent rheology and the extended Boussinesq approximations.

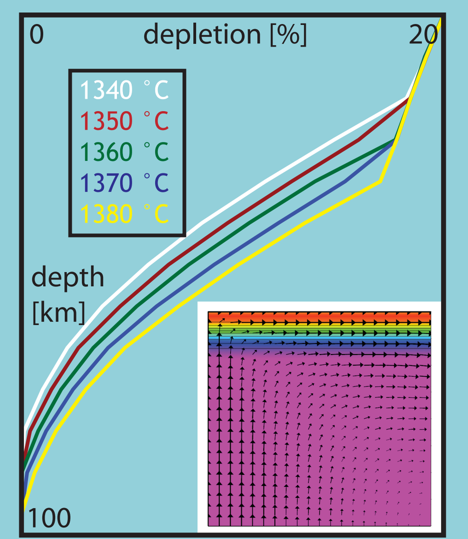

Fig. 6: The initial profile of depletion due to ridge melting is self-consistently calculated in 2D-cornerflow models for the parameters applied in the simulation.

Melting

Fig. 7: The peridotite melting applied was scaled by Katz et al. 2003. Water significantly reduces the solidus only at small degrees of melting, as it is preferentially dissolved in the liquid. When the porosity reaches a critical value (~1%), melt extraction ensues incompatible water is removed. Subsequently, the melting model quickly approaches the dry case.

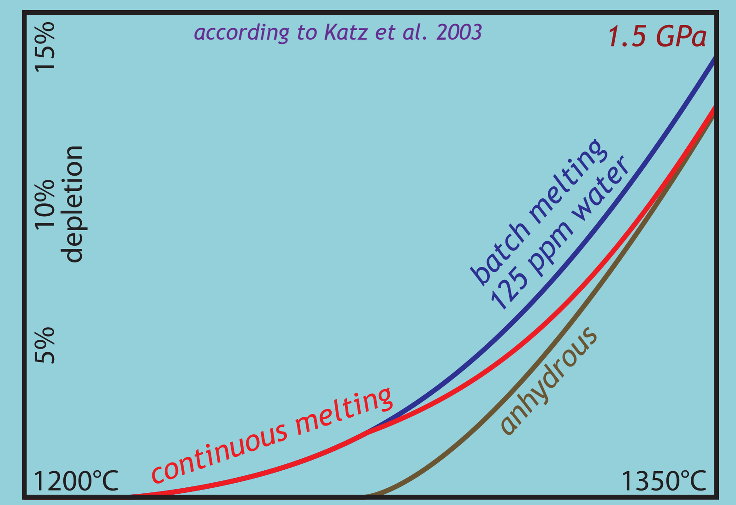

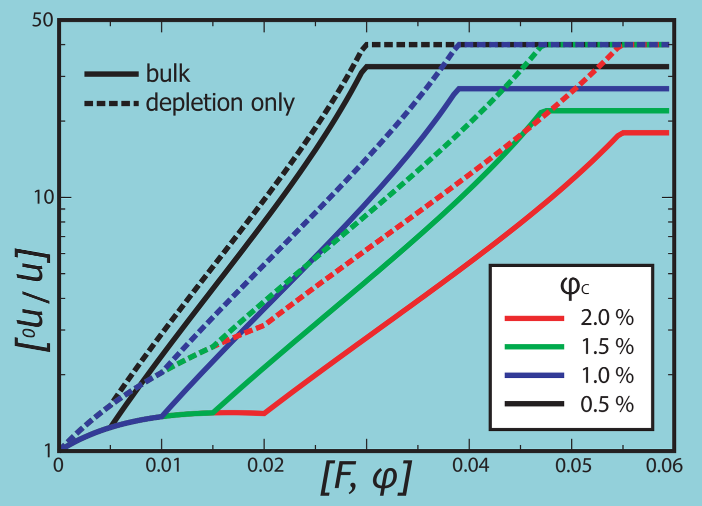

Fig. 8: The viscosity jump versus depletion F and melt content φ for different critical porosities φ_c with compositional rheology. Dehydration during partial melting increases the intrinsic viscosity of peridotite. We assume a viscosity jump of 40 for total extraction of water. Melt lubrication is unable to compensate for stiffening due to dehydration for any realistic φ_c.

Results

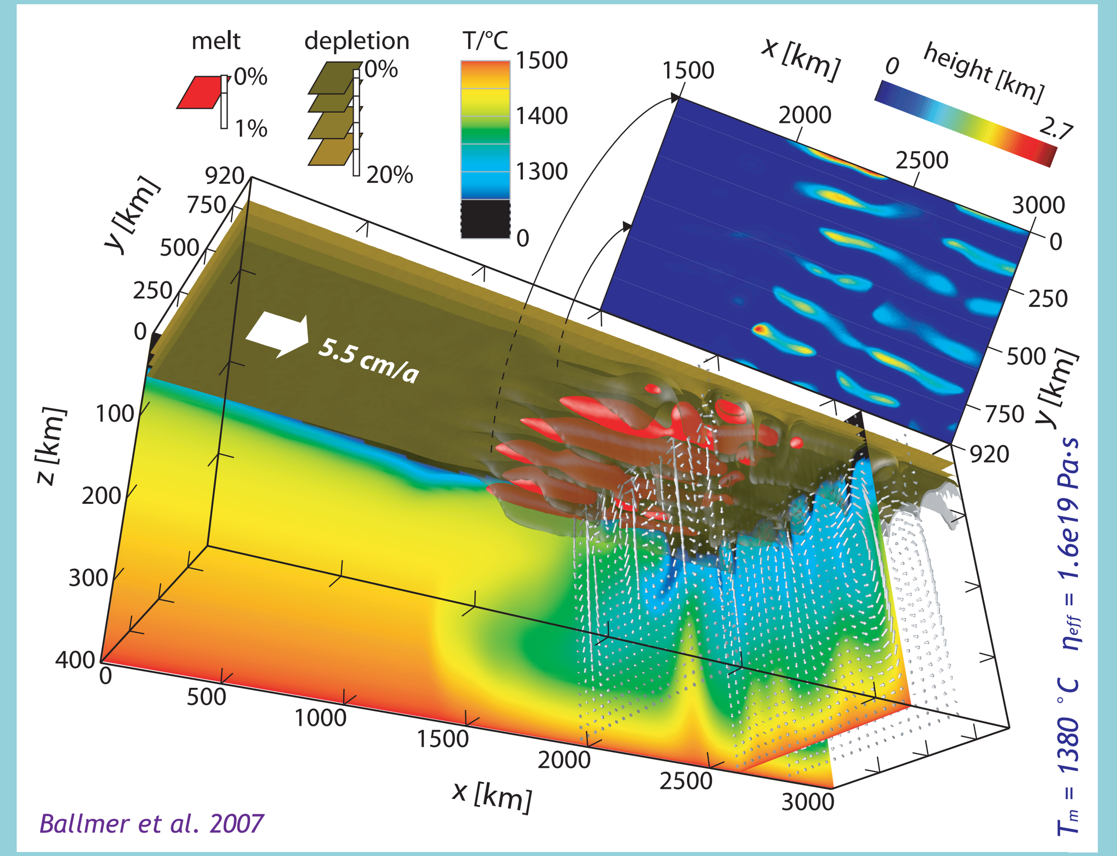

Fig. 9: Isosurfaces (melt fraction and depletion), and X-sections of the T-field for an example case. Lifted from the top is a plan view of the thickness of extracted melt accumulated on an overriding plate. When small-scale convection initiates, the depleted lid is removed in downwelling sheets parallel to plate-motion. Hence, upwelling returnflow advects hot and undepleted material triggering melting within elongated anomalies. Crustal thicknesses predicted for seamounts are realistic. (see also values in dark red in *Fig. 11*).

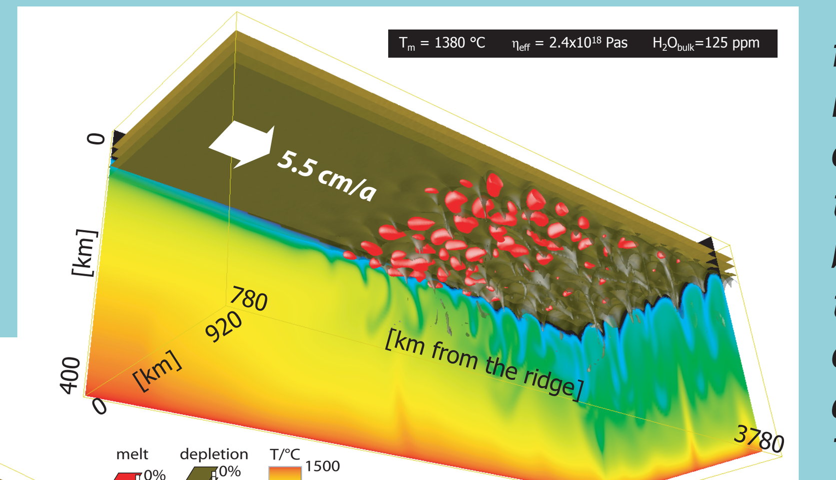

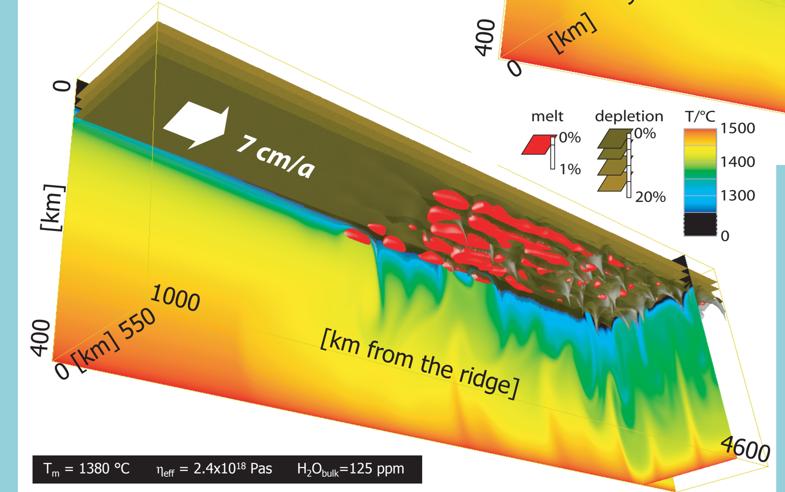

Fig. 10: When taking into account that the rheology is dependent on melt and water content, viscosity has to be about 7-fold lower to maintain the same onset ages and similar amounts of melting. This is because of a dehydrated and hence stiff harzburgite layer from MOR-melting. The style of convection is sensitive to the speed of plate motion. Thus, only for fast plates the geometry of melting remains like in *Fig. 9*. The duration of associated volcanism is large, as the asthenosphere cools relatively slow.

Discussion

Fig. 11: The seafloor ages, over which volcanism occurs, correlate positively with both mantle temperature (T_m) and viscosity (η_{eff}). Higher η_{eff} delays melting due to a sluggish convection, and so does as well larger T_m due to the stabilizing effect of a thicker residue from previous mid-ocean ridge melting. The duration of volcanism is ~10 Myr. With volcanic chains forming over such an elongated anomaly, age-distance relationships are not implicitly linear.

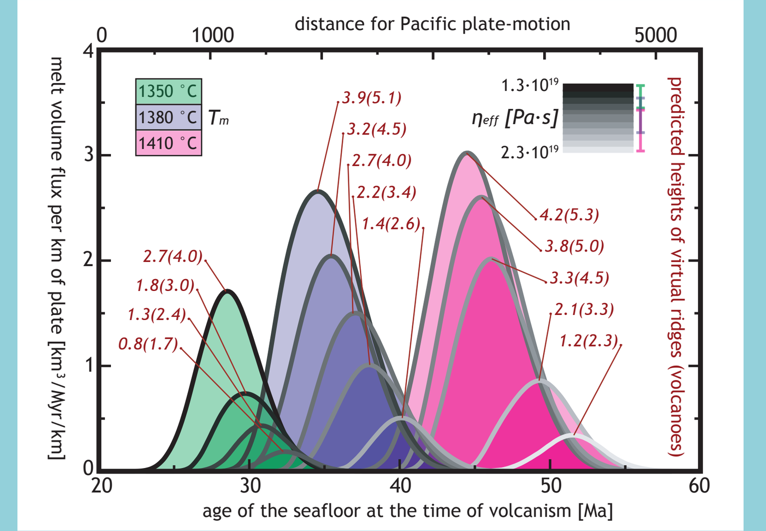

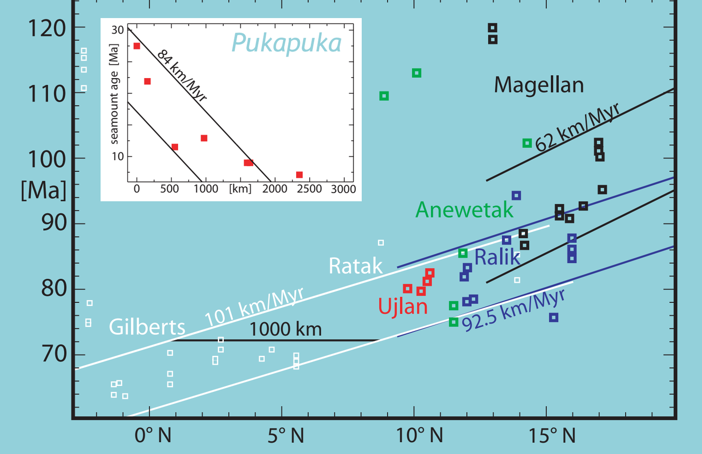

Fig. 12: Radiometric ages from the Marshall Islands and Pukapuka ridges can be reconciled with volcanism formed over an elongate anomaly. Apparent age progression of this anomaly may be about plate speed (black lines) or faster, if the anomaly systematically propagates towards younger ages.

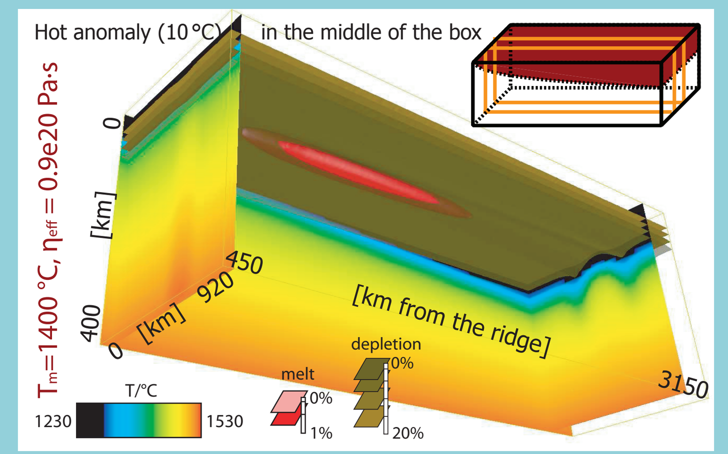

Fig. 13: A small lateral (thermal or compositional) anomaly may focus volcanism into a single ridge. In this realistic case, the onset of the instability is reduced adjacent to the heterogeneity. Thus, effective mantle viscosity required for generating significant partial melting is larger. Since the distribution and wavelength of any heterogeneity is expected to be strongly time-dependent, onset ages of convection vary through time, what leads to further complexities of age-distance relationships predicted.

Conclusion

- Melting due to small-scale convection works for average mantle temperatures and low but still realistic viscosities.
- Melting anomalies are elongated (~1000 km), and therefore, the associated volcanic chains display irregular age-distance relationships.
- The age of the seafloor, on which volcanism occurs (25-55 Myr) is predominantly related with mantle temperature, whereas the amount of volcanism is mainly dependent on effective viscosity.
- Dehydration rheology reduces the viscosity required for volcanism and increases the duration of melting.
- Lateral density heterogeneity increases the viscosity required for volcanism and reduces the onset age of small-scale convection.